

Supplementary data for the article:

Antonijević, I. S.; Janjić, G. V.; Milčić, M. K.; Zarić, S. D. Preferred Geometries and Energies of Sulfur-Sulfur Interactions in Crystal Structures. *Crystal Growth and Design* **2016**, *16* (2), 632–639. <https://doi.org/10.1021/acs.cgd.5b01058>

Supporting Information

Preferred geometries and energies of sulfur-sulfur interactions in crystal structures

Ivana S. Antonijević, Goran. V. Janjić, Miloš. K. Milčić, Snežana. D. Zarić

The methanethiol structure is optimized using MP2 method and cc-pVQZ basis set. The theoretical IR spectrum is shown on Figure S1.

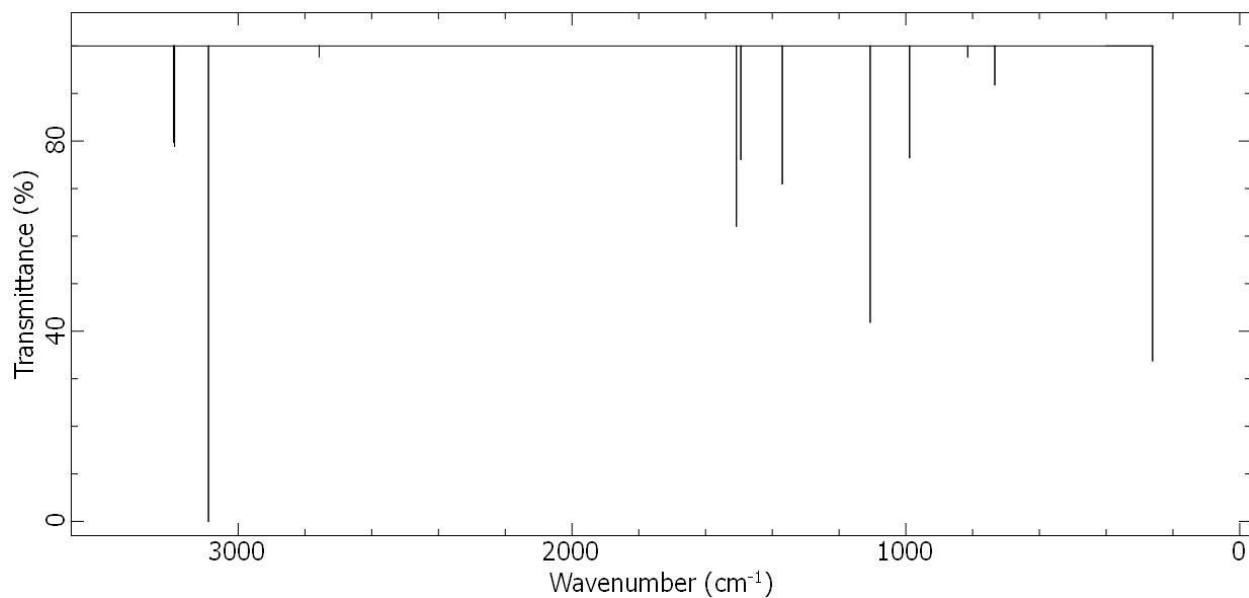


Figure S1. IR spectrum for optimized geometry of methanethiol molecule (monomer)

Vibrational frequencies for optimized geometry of methanethiol molecule (Table S1) have only positive values, which confirms that optimized geometries are correct.

Table S1. Vibrational frequencies and intensities of IR spectrum of methanethiol molecule

| Frequencies (cm ⁻¹) | Intensities |
|---------------------------------|-------------|
| 261.113 | 66.215 |
| 733.511 | 818.686 |
| 814.441 | 229.189 |
| 988.797 | 235.252 |
| 1106.73 | 581.061 |
| 1370.06 | 290.035 |
| 1494.27 | 23.886 |
| 1507.57 | 379.186 |
| 2757.18 | 227.672 |
| 3088.91 | 100.000 |
| 3190.49 | 210.989 |
| 3193.34 | 20.284 |

Results of CCSD(T)/CBS calculations of interaction energy are presented in Table S2. CCSD(T)/CBS interaction energies are calculated by applying the extrapolation scheme of Makie for different orientations of two methanethiol molecules to find the minima on CCSD(T) potential curve by varying the value of normal distance (equilibrium distance) R. In the Table S2 are three sets of R values (R_1 , R_{\min} and R_2); R_1 values are 0.5 Å greater than R_{\min} , and R_2 values are 0.5 Å smaller than R_{\min} values for all model systems. In this way, we show the equilibrium (R_{\min}) distances for the minima on the CCSD(T) potential curve.

Table S2. Calculated CCSD(T)/CBS energy values and normal distances R for all examined model systems

| Model | R_1 (Å) | E_{int} CCSD(T) (kcal/mol) | R_{\min} (Å) | E_{int} CCSD(T) (kcal/mol) | R_2 (Å) | E_{int} CCSD(T) (kcal/mol) |
|----------|-----------|--|----------------|--|-----------|--|
| A | 4.0 | -0.45 | 4.5 | -0.52 | 5.0 | -0.38 |
| B | 3.6 | -0.08 | 4.1 | -0.72 | 4.6 | -0.60 |
| C | 3.4 | -0.46 | 3.9 | -1.80 | 4.4 | -1.35 |
| D | 3.5 | -0.11 | 4.0 | -0.37 | 4.5 | -0.18 |
| E | 3.1 | 0.07 | 3.6 | -2.20 | 4.1 | -1.82 |

Table S3. Refcode list of crystal structures used for statistical analysis of data obtained from the CSD.

| | | | | | | | |
|-----|----------|-----|----------|-----|----------|------|----------|
| 1. | NALCYS19 | 30. | BOQCUF04 | 59. | HORZAQ | 88. | PAGYIG |
| 2. | NALCYS20 | 31. | BOQCUF05 | 60. | HORZEU | 89. | PAMVUV |
| 3. | NALCYS21 | 32. | BOQCUF06 | 61. | HORZIY | 90. | POHJON01 |
| 4. | NALCYS22 | 33. | BOQCUF07 | 62. | HORZOE | 91. | PUVWIM |
| 5. | NALCYS23 | 34. | BOQCUF08 | 63. | HUKJUT | 92. | QEKXOT |
| 6. | NALCYS24 | 35. | BOQCUF09 | 64. | ICAKEC | 93. | QEKXUZ |
| 7. | NALCYS25 | 36. | BOQCUF10 | 65. | ICAKIG | 94. | QEKYAG |
| 8. | NALCYS26 | 37. | BOWKOO | 66. | IFUJID | 95. | QEKYEK |
| 9. | NALCYS27 | 38. | BOWKOO01 | 67. | KEXNOR | 96. | QEKYIO |
| 10. | NALCYS28 | 39. | BOWKOO02 | 68. | KUKGAZ | 97. | QEKYOU |
| 11. | VEDCOW01 | 40. | BOWKOO03 | 69. | LCYSTN04 | 98. | QEKYUA |
| 12. | YOJXOM | 41. | BOWKOO04 | 70. | LCYSTN22 | 99. | QEKZAH |
| 13. | YOJXOM01 | 42. | BOWKOO05 | 71. | LCYSTN23 | 100. | SOMYEZ |
| 14. | YOJXOM02 | 43. | BOWKOO06 | 72. | LCYSTN24 | 101. | TAXMUA |
| 15. | YOJXOM03 | 44. | BOWKOO07 | 73. | LCYSTN25 | 102. | TERTEP |
| 16. | YOJXOM04 | 45. | BOWKOO08 | 74. | LOCJET | 103. | UDUVUL |
| 17. | YOJXOM05 | 46. | CEDYEQ | 75. | LOCJET01 | 104. | VEDCOW |
| 18. | YOJXOM06 | 47. | CEJTEQ | 76. | LOCJET02 | 105. | VEZLOC |
| 19. | YOJXOM07 | 48. | CYSCLM11 | 77. | LOCJET03 | 106. | VINWUM |
| 20. | YOJXOM08 | 49. | DIXFAS | 78. | LOCJET04 | 107. | VOPBEH |
| 21. | YOJXOM09 | 50. | FEDQIP | 79. | LOCJET05 | 108. | WAQFEZ |
| 22. | YOJXOM10 | 51. | FENJUD | 80. | LOCJET06 | 109. | WEGDES |
| 23. | ADIXOA | 52. | GLUTAS02 | 81. | LOCJET07 | 110. | WESZUQ |
| 24. | BARPOB | 53. | GLUTAS03 | 82. | LOCJET08 | 111. | WOGRIT |
| 25. | BEQPUI | 54. | GLUTAS04 | 83. | LOCJET09 | 112. | WUQZAJ |
| 26. | BOQCUF | 55. | GLUTAS05 | 84. | LOCLOF | 113. | XAFVEH |
| 27. | BOQCUF01 | 56. | GLUTAS06 | 85. | LOCLOF01 | 114. | XIJKIK01 |
| 28. | BOQCUF02 | 57. | GOMDAN | 86. | NALCYS17 | 115. | XUHLOC |
| 29. | BOQCUF03 | 58. | HESTAB | 87. | OWADUM | 116. | YAJHEW |

Energies of interactions. The methods for potential curve calculations were chosen because they are in agreement with the CCSD(T) energies on limit. These methods have similar energy values with energy values obtained by CCSD(T) method, which is considered as golden standard

in quantum chemistry (deviation is less than 10%). The single point calculations on potential curves were done with TPSS-D3/aug-cc-pVDZ method for parallel model systems (A, B and C), with TPSS-D3BJ/aug-cc-pVDZ method for model system with normal orientation (D), and with MP2/cc-pVQZ method for model system E (Table S4).

Table S4. Comparison of interaction energy values calculated using different quantum chemical methods with the energy values calculated at CCSD(T)/CBS level

| Model system | $\Delta E_{\text{CCSD(T)}}$ (kcal/mol) | $\Delta E_{\text{interaction}}$ (kcal/mol) |
|---------------------|--|--|
| A | -0.52 | -0.57 ^a |
| B | -0.72 | -0.78 ^a |
| C | -1.80 | -1.81 ^a |
| D | -0.37 | -0.33 ^b |
| E | -2.20 | -2.19 ^c |

^a TPSS-D3/aug-cc-pVDZ

^b TPSS-D3BJ/aug-cc-pVDZ

^c MP2/cc-pVQZ

Single point calculations were performed for different offsets (r) along three directions (Figure S2).

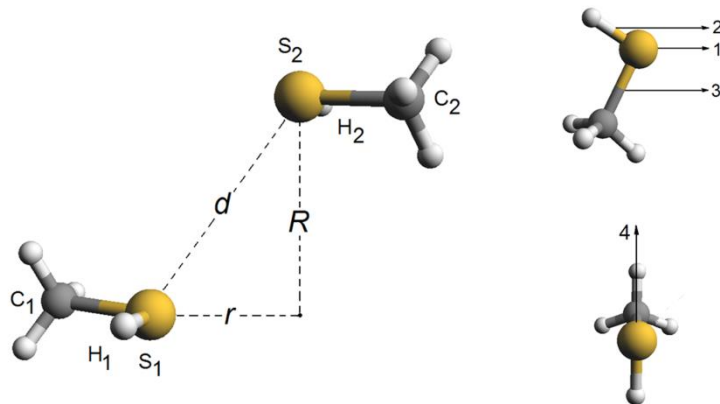


Figure S2. The parameters that were used for quantum chemical calculations.

For the geometries of the parallel orientation (model systems A to C, Figure 9) the monomer geometries were kept rigid, while the normal distance R was systematically varied to find the R with the strongest interaction. In the model systems D and E the distance d between two sulfur atoms was systematically changed. Model system A was moved along direction 1, model system B along direction 2, model system C along direction 3.

The potential-energy curves for different methanethiol dimers (Figure S3-S7) were additionally calculated with TPSS-D3 method and aug-cc-pVDZ basis set for model systems with parallel orientation (A-C), and using the same functional but with Becke-Johnson damping (TPSS-D3BJ/aug-cc-pVDZ) for model system with normal orientation D. Interaction energies for model system E with maximized electrostatic interaction was calculated using MP2 method and cc-pVQZ basis set. The energies were corrected by the basis set superposition error (BSSE) using the Counterpoise method.

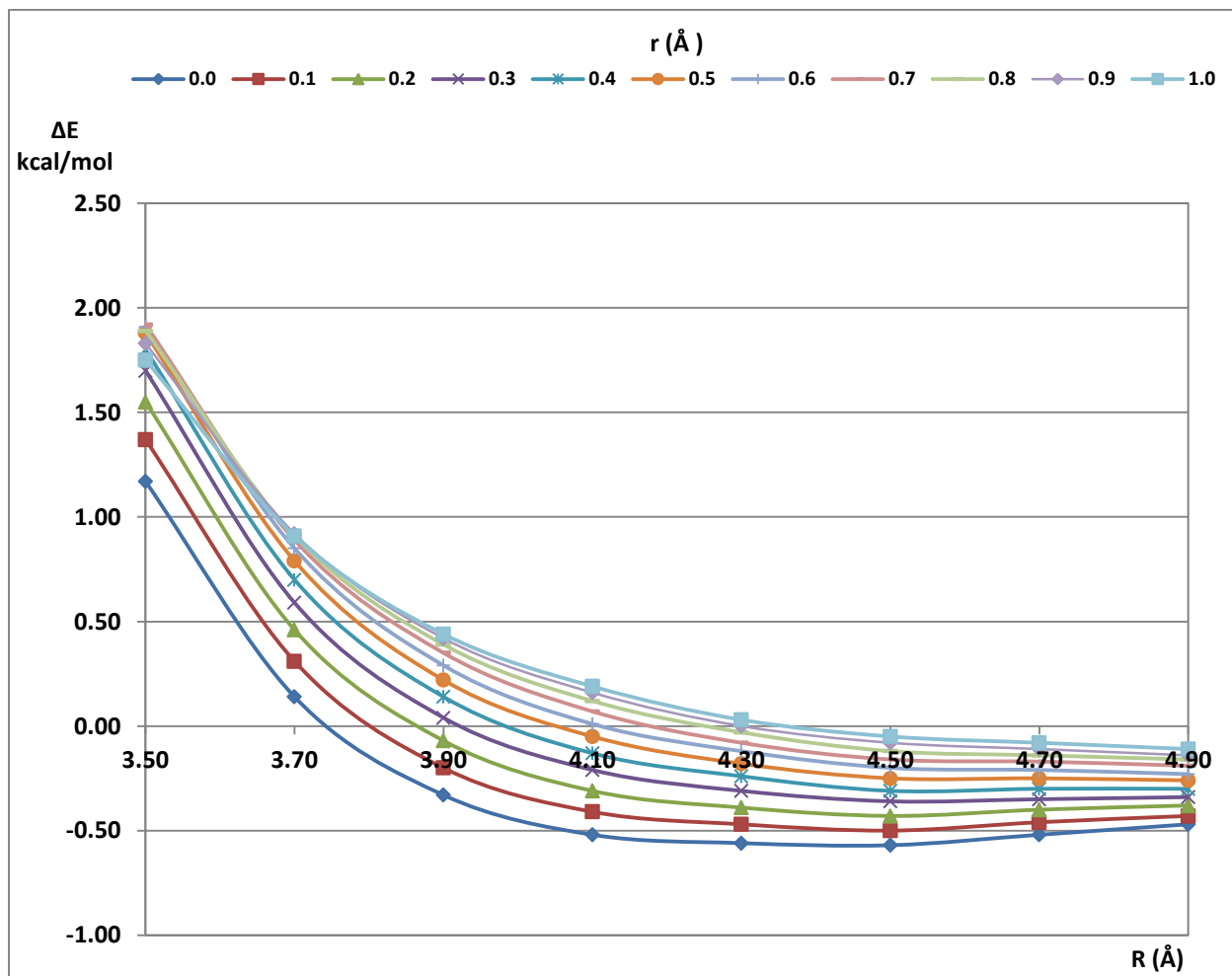


Figure S3. Graph of the S...S interaction energy versus height (R) for different offset (r) values for model system A.

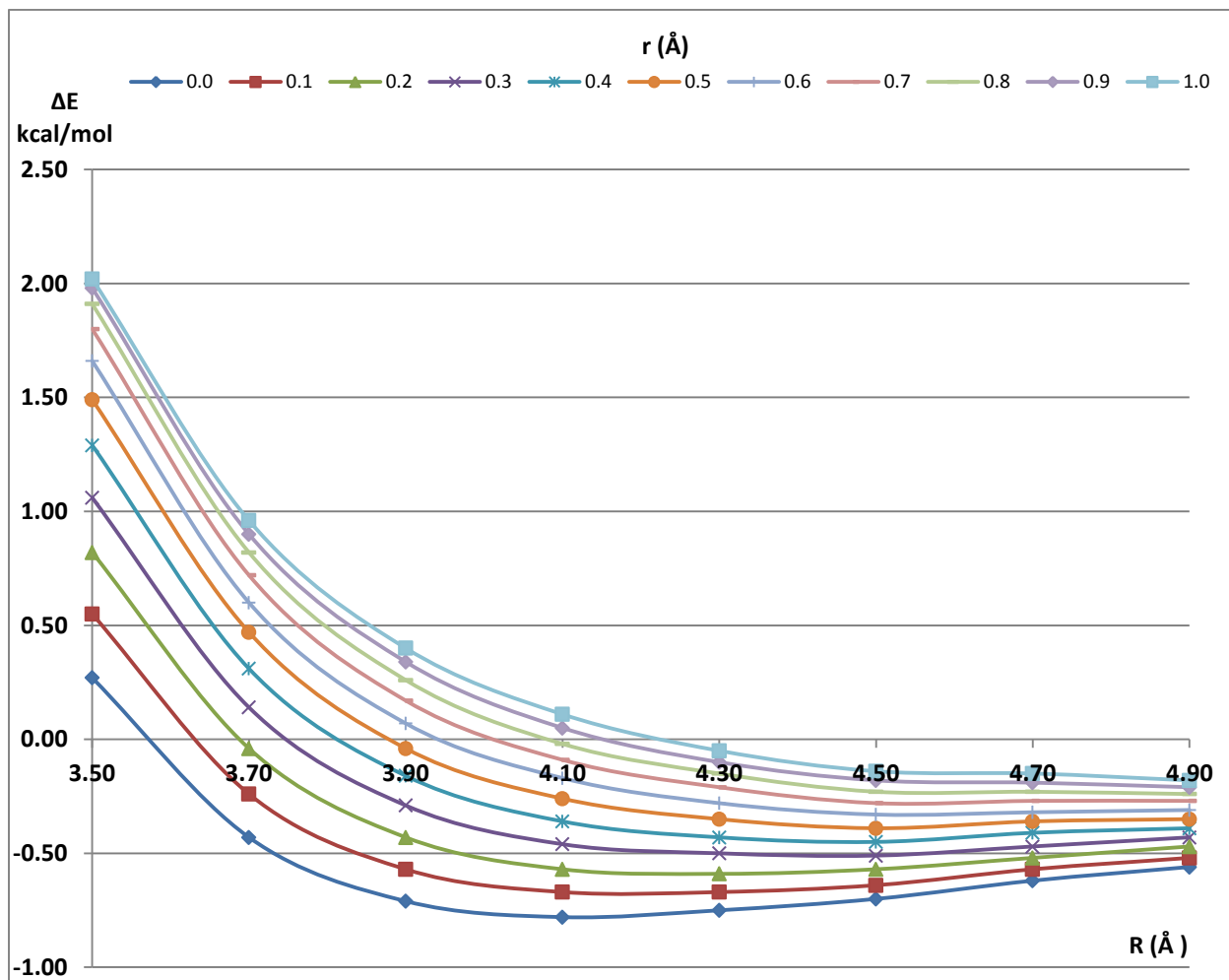


Figure S4. Graph of the S...S interaction energy versus height (R) for different offset (r) values for model system B.

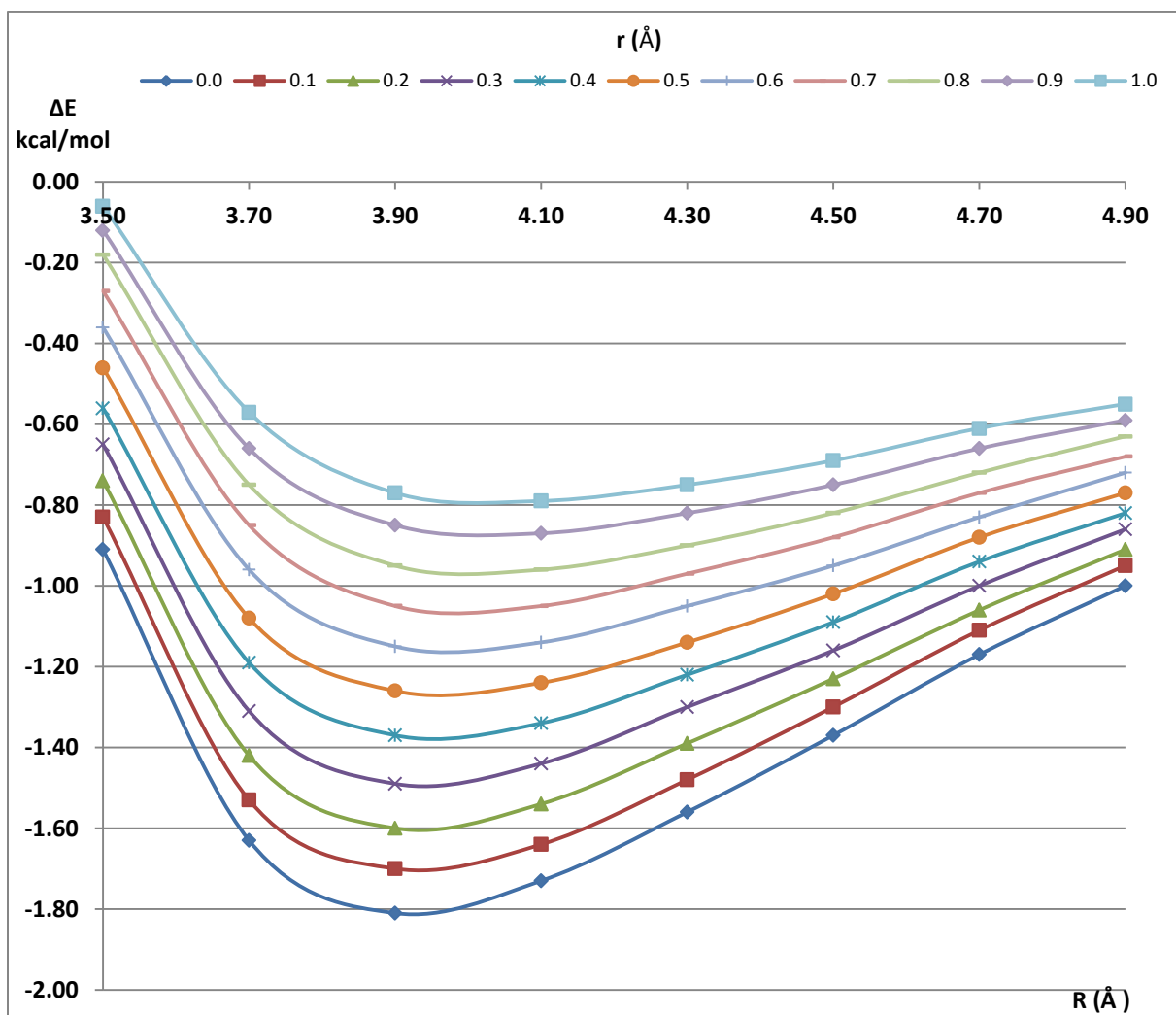


Figure S5. Graph of the S...S interaction energy versus height (R) for different offset (r) values for model system C.

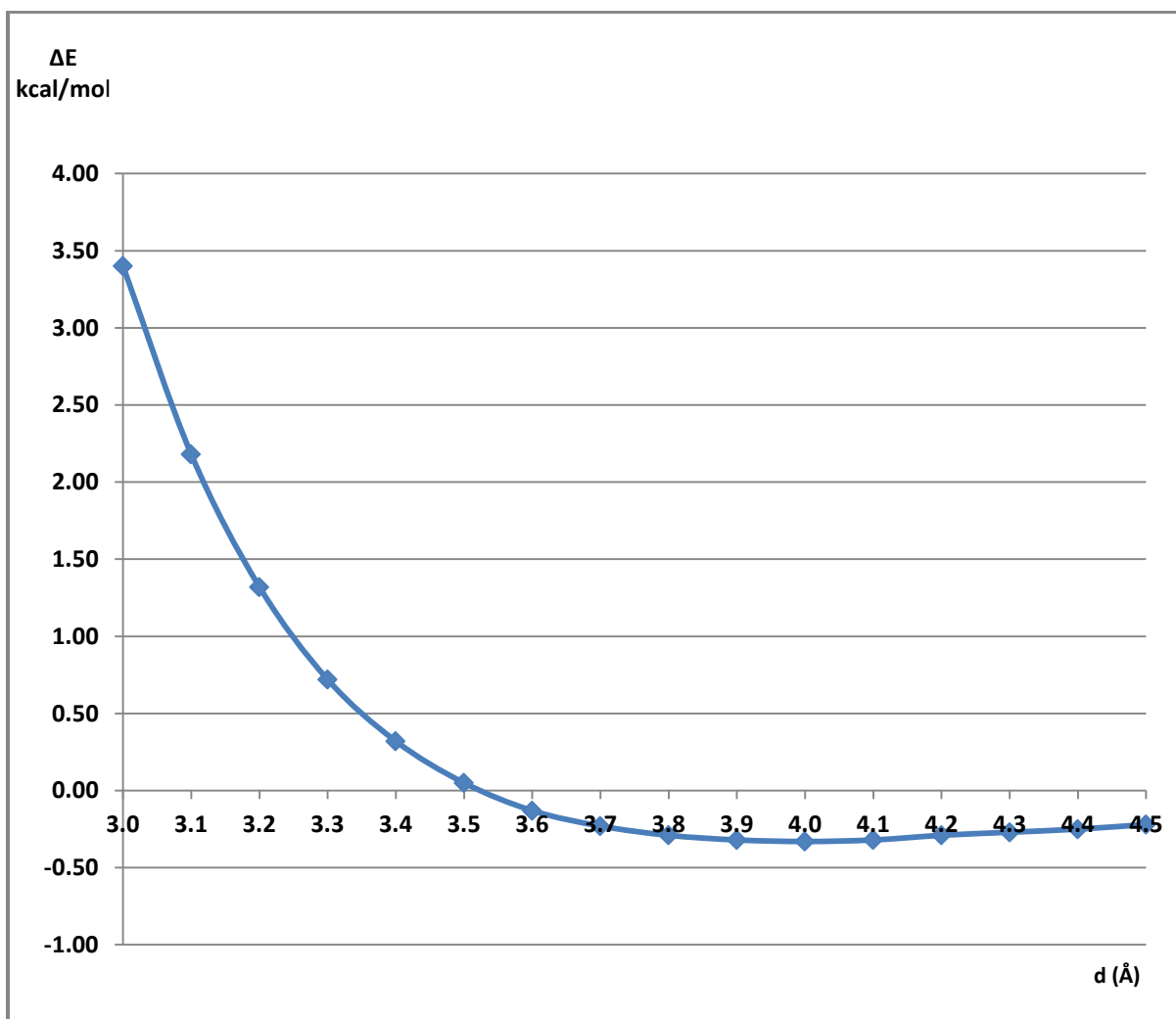


Figure S6. Graph of the S...S interaction energy versus S...S distances (d) for model system D.

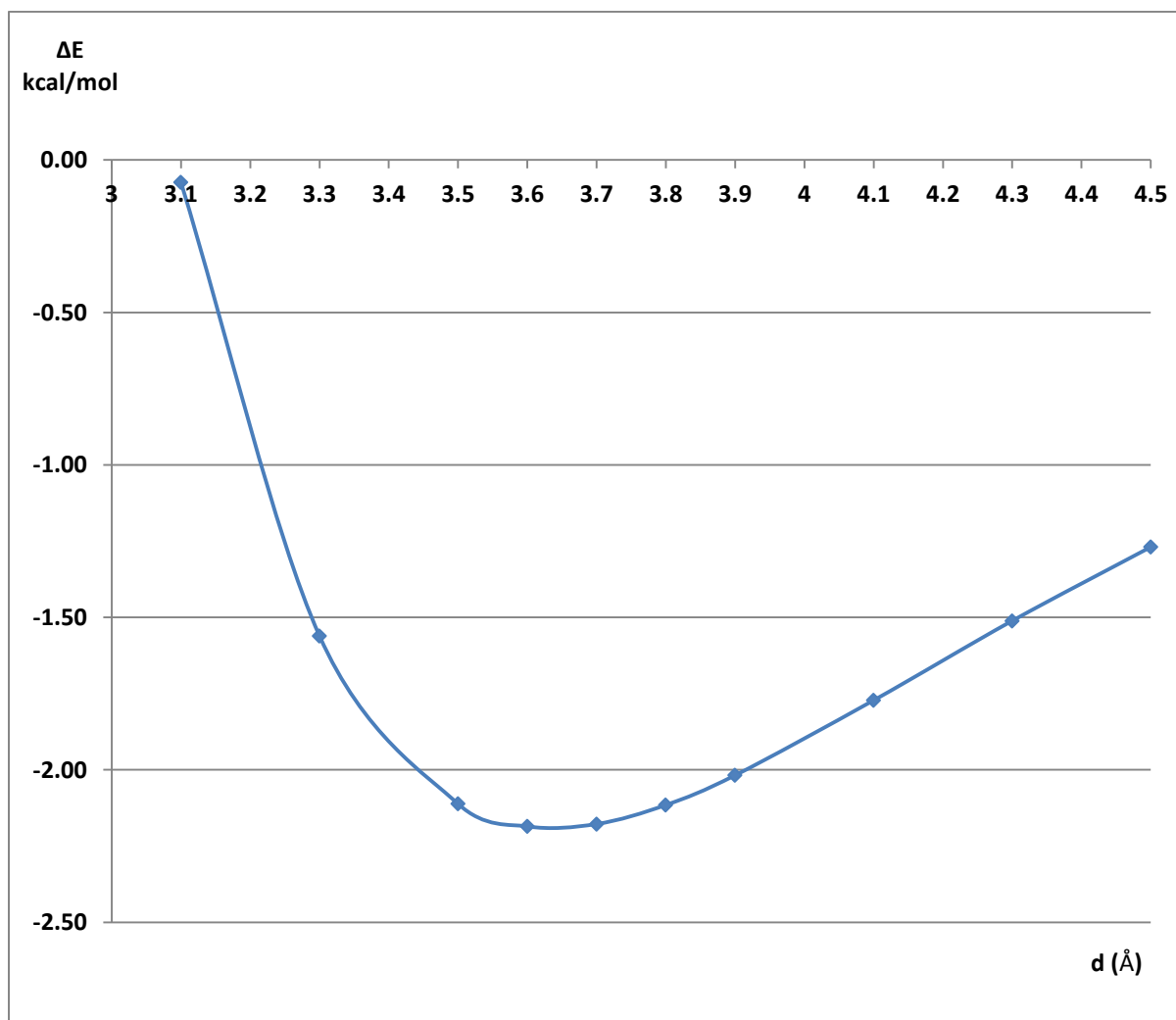


Figure S7. Graph of the S...S interaction energy versus S...S distances (d) for model system E.

Cartesian (XYZ) coordinates for most stable orientations of studied model systems.

Table S5. Cartesian coordinates for model system A

| atom | X | Y | Z |
|------|-----------|-----------|-----------|
| H | -2.09983 | 0.965885 | 1.226844 |
| S | -2.126744 | 0.729198 | -0.087747 |
| C | -2.718016 | -0.982387 | 0.019353 |
| H | -2.013526 | -1.611753 | 0.553037 |
| H | -3.697465 | -1.0344 | 0.483249 |
| H | -2.798534 | -1.340226 | -1.002833 |
| S | 2.126757 | -0.729202 | 0.087748 |
| H | 2.099842 | -0.96589 | -1.226844 |
| C | 2.718028 | 0.982383 | -0.019353 |
| H | 2.798546 | 1.340222 | 1.002833 |
| H | 3.697325 | 1.034428 | -0.483565 |
| H | 2.013376 | 1.611824 | -0.552733 |

Table S6. Cartesian coordinates for model system B

| atom | X | Y | Z |
|------|-----------|-----------|-----------|
| H | 1.700299 | 0.903612 | 1.219593 |
| S | 1.938082 | 0.744669 | -0.085433 |
| C | 2.623444 | -0.930988 | 0.028796 |
| H | 3.524317 | -0.949705 | 0.633198 |
| H | 1.892556 | -1.63174 | 0.418633 |
| H | 2.8791 | -1.224133 | -0.985158 |
| S | -1.936226 | -0.74548 | 0.073991 |
| H | -1.706865 | -0.883038 | -1.234966 |
| C | -2.625765 | 0.930309 | -0.008855 |
| H | -2.875222 | 1.206664 | 1.011339 |
| H | -1.899051 | 1.63871 | -0.392627 |
| H | -3.530895 | 0.956677 | -0.606575 |

Table S7. Cartesian coordinates for model system C

| atom | X | Y | Z |
|------|-----------|-----------|-----------|
| H | -1.880214 | 0.943565 | 1.227856 |
| S | -1.870472 | 0.708419 | -0.087251 |
| C | -2.115174 | -1.085877 | 0.018677 |
| H | -1.297238 | -1.566397 | 0.545276 |
| H | -3.062001 | -1.329019 | 0.489447 |
| H | -2.13209 | -1.45081 | -1.004031 |
| S | 1.870485 | -0.708421 | 0.08725 |
| H | 1.880227 | -0.943565 | -1.227857 |
| C | 2.115186 | 1.085875 | -0.018675 |
| H | 2.132102 | 1.450807 | 1.004034 |
| H | 3.061857 | 1.329021 | -0.489759 |
| H | 1.297078 | 1.566437 | -0.544968 |

Table S8. Cartesian coordinates for model system D

| atom | X | Y | Z |
|------|-----------|-----------|-----------|
| H | 2.030026 | -1.963147 | -1.068083 |
| S | 0.984203 | -1.741076 | -0.266937 |
| C | 0.984203 | -3.368676 | 0.534008 |
| H | 0.811676 | -4.163244 | -0.184408 |
| H | 1.908076 | -3.543242 | 1.075497 |
| H | 0.162448 | -3.357613 | 1.243933 |
| S | -0.984203 | 1.741076 | -0.266937 |
| H | -2.030026 | 1.963147 | -1.068083 |
| C | -0.984203 | 3.368676 | 0.534008 |
| H | -0.162448 | 3.357613 | 1.243933 |
| H | -0.811676 | 4.163244 | -0.184408 |
| H | -1.908076 | 3.543242 | 1.075497 |

Table S9. Cartesian coordinates for model system E

| atom | X | Y | Z |
|------|-----------|-----------|----------|
| H | 0.00000 | 0.00000 | 0.00000 |
| S | 0.00000 | 0.00000 | 1.336 |
| C | 1.801832 | 0.00000 | 1.545754 |
| H | 2.250023 | -0.890683 | 1.117929 |
| H | 2.249987 | 0.890849 | 1.118238 |
| H | 1.982756 | 0.00000 | 2.616577 |
| S | 0.00000 | 0.00000 | 4.936 |
| H | -0.891877 | 0.994712 | 4.936 |
| C | -1.206255 | -1.354823 | 4.936 |
| H | -0.629317 | -2.274898 | 4.936 |
| H | -1.825254 | -1.333533 | 4.045151 |
| H | -1.825486 | -1.333327 | 5.826683 |

Quantum Theory of Atoms In Molecules (QTAIM) analysis and NCI index. The electron density for QTAIM analysis¹ was obtained from MP2/aug-cc-pVQZ calculation on previously modeled the most stable dimer geometry. QTAIM analysis on electron density topology was done with MultiWfn program.² Image of electron density contour map with critical points is created with AIMALL program.³ The NCI index and reduced density gradient were calculated with NCIPLOT program.⁴

QTAIM analysis. QTAIM analysis of the model system E wave function has shown the existence of three critical points between monomers (Figure S8). Two of the CP's corresponds to bond critical points (BCP) and one to the ring critical point (RCP).

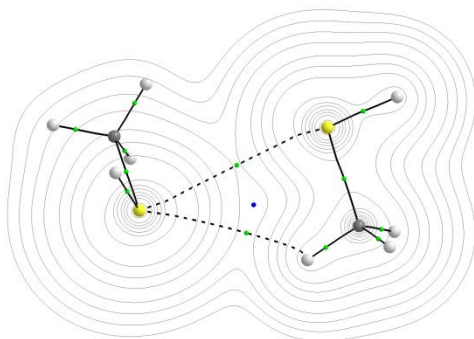


Figure S8. Electron density contour map for dimer. Large spheres represent atoms: C - gray, S - yellow and H - white. Small spheres represent critical points: BCPs in green and RCP in blue

This point can be further strengthening with Quantum Atoms in Molecule (QTAIM) and NCI index analysis of model system E. QTAIM analysis of the model system E wave function has shown the existence of two bond critical points (BCP) between molecules. The first BCP occurs between two sulfur atoms and the second between sulfur and hydrogen atom (Figure S9). Properties of electron density calculated at these critical points are shown in Table S10. The electron density at the BCP1 is larger than at the BCP2 indicating that sulfur-sulfur interaction is most responsible for the binding in model system E.

Table S10. Properties of electron density calculated at CP's with QTAIM method for model system E.

| | ρ^a | $\nabla^2\rho^b$ | $\text{Sign}(\lambda_2)^c$ | V_c^d | G_c^e | H_c^f |
|------|----------|------------------|----------------------------|-----------|----------|----------|
| BCP1 | 0.007761 | 0.020317 | — | -0.003752 | 0.004416 | 0.000664 |
| BCP2 | 0.006572 | 0.019267 | — | -0.003352 | 0.004084 | 0.000733 |
| RCP | 0.005883 | 0.019532 | + | -0.003140 | 0.004011 | 0.000872 |

^a electron density at CP

^bLaplacian of electron density at CP

^c Sign of the second eigenvalue of the electron density Hessian matrix at CP

^d electronic potential energy density at CP

^e electronic kinetic energy density at CP

^f total electron energy density at CP

NCI index. To confirm QTAIM analysis results the calculations of reduced density gradient was performed. The reduced density gradient, coming from the density and its first derivative ($s=1/[2(3\pi^2)^{1/3}]|\nabla\rho|/\rho^{4/3}$), is a dimensionless quantity used to describe the deviation from a

homogeneous electron distribution. Regions where the electron density $\rho(r)$ and reduced density gradient s are low correspond to regions where non-covalent interactions occur. The plot of the reduced density gradient versus the electron density multiplied by the sign of the second Hessian eigenvalue ($sign(\lambda_2)\rho$) (Figure S9) indicates two low gradient low density regions. The booth BCP's lies in the negative $sign(\lambda_2)\rho$ part and RCP is in the positive $sign(\lambda_2)\rho$ part.

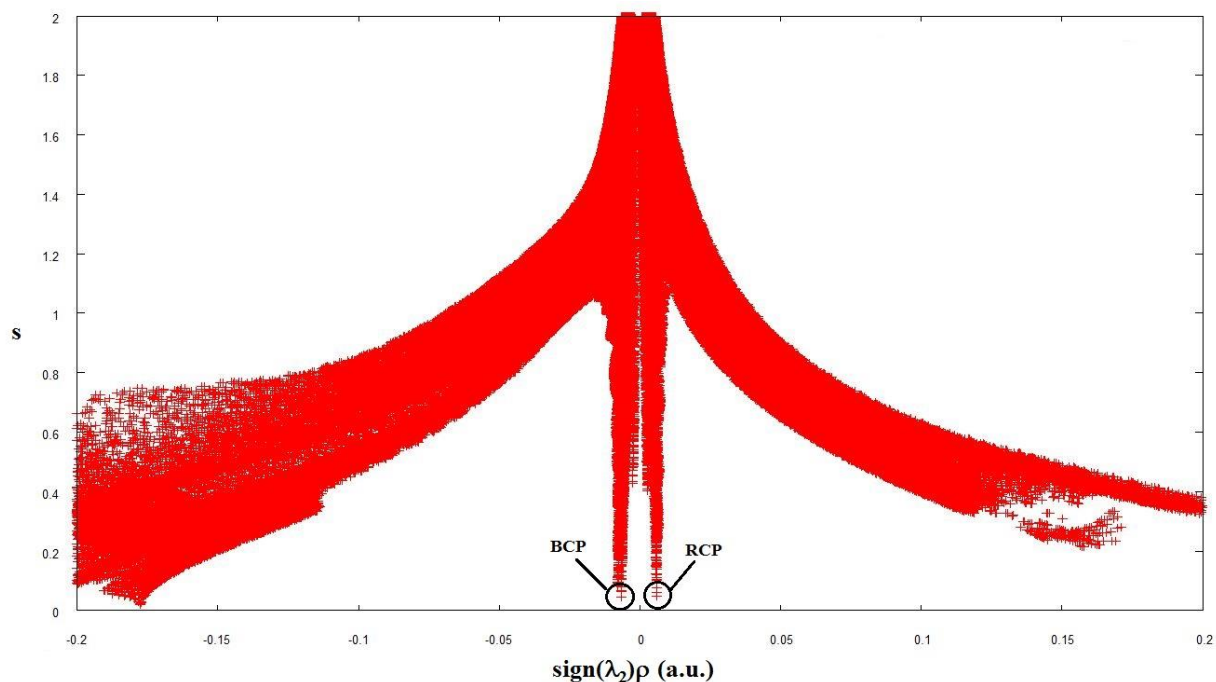


Figure S9. Plot of the reduced density gradient s and $sign(\lambda_2)\rho$ for model system E.

On the Figure S10 a two NCI isosurfaces can be distinguished. The first NCI isosurface lies between two sulfur atoms and is disk-shaped and blue in color indicating an attractive and very localized interaction. At the center of this region lies BCP1. The second NCI isosurface lies between sulfur atom and CH_3 group. The interaction is repulsive near the center of the S-S-C-H ring (red region) and weakly attractive in the region between sulfur and hydrogen atoms. The RCP lies in the repulsive and BCP2 in the attractive region.

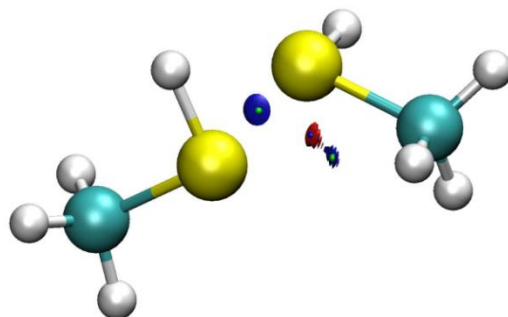


Figure S10. Plot of NCI isosurfaces for model system E. A continuous color-coding scheme is used; attractive interactions are represented in blue and repulsive interactions in red. Small spheres represent critical points: BCPs -green, RCP – blue.

REFERENCES

- (1) Biegler-König, F. W.; Bader, R. F. W.; Tang, T. H. *J. Comput. Chem.* **1982**, *3*, 317–328.
- (2) Lu, T.; Chen, F. W. *J. Comput. Chem.* **2012**, *33*, 580–592.
- (3) AIMAll (Version 15.05.18), Keith, T. A., TK Gristmill Software, Overland Park KS, USA, **2015** (aim.tkgristmill.com)
- (4) Contreras-García, J.; Johnson, E. R.; Keinan, S.; Chaudret, R.; Philip, Piquemal J.; Beratan, D. N.; Yang, W. *J. Chem. Theory Comput.* **2011**, *7*, 625–632.